Recent experimental results from the relativistic heavy-ion collisions at LHC and RHIC

Ilya Selyuzhenkov[1]
Research Division and ExtreMe Matter Institute EMMI,
GSI Helmholtzzentrum für Schwerionenforschung
Planckstraße 1 64291 Darmstadt, Germany

A new era has started in the field of relativistic heavy-ion physics with lead beams delivered by the Large Hadron Collider (LHC) in November 2010. In this proceedings I highlight the main results from experimental measurements with Pb–Pb collisions at the incident energy of 2.76 TeV/nucleon recorded by the LHC experiments. Recent experimental developments from the Relativistic Heavy Ion Collider (RHIC) at the GeV incident energy scale are also discussed. All together LHC and RHIC measurements provide new insights on the properties and features of the new hot and dense form of matter created in the course of the relativistic heavy-ion collision.

1 Introduction

The main goal of the more than a ten years of operation of the Relativistic Heavy Ion Collider (RHIC), and of the heavy-ion program recently launch at the Large Hadron Collider (LHC) is to study the properties of the hot and dense matter, the so called quark-gluon plasma (QGP), which is believed to have existed a few microseconds after the big bang. By colliding heavy nuclei at relativistic energies we heat up the normal cold matter and transfer it from the hadronic phase to fireball of deconfined quarks and gluons, which allows us to probe the QGP properties in the laboratory.

Theoretically the time evolution of the system created in the course of heavy-ion collisions is described by a sequence of several stages. It starts from the initial pre-equilibrium state when hard parton scattering occurs and gluonic fields are formed. The next stage is the formation and then expantion of a thermalized state of matter, the quark-gluon plasma, which is conventionally described by hydrodynamics. Consequently, the quarks and gluons are coupled (hadronize) into hadrons, which ends with the phase of chemical and then kinetic freeze out (all interactions are ceased at this moment). The only data which directly accessible for experimentalist is the information on this last hadronic stage. Evidently, it

[1]ilya.selyuzhenkov@gmail.com

is not possible to constrain theoretical models which pretend to describe the evolution of the heavy-ion collision and identify the one which most precisely reflects the nature of the collision with a single measurement, and so it is necessary to study many experimental observables to pin down the properties of the QGP.

In this proceedings I highlight the new results from the ALICE, CMS, and ATLAS Collaborations from the first heavy-ion run at LHC in November 2010, as well as recent experimental developments by the STAR and PHENIX Collaborations at RHIC. I start with a discussion of global properties of the collisions at LHC energies, such as charged hadrons multiplicity, particle yields, and a measurement of the collision freeze out volume from the Bose-Einstein correlations of identical pions. I then briefly review the results for anisotropic flow which reflect collectivity in particles production and allows us to experimentally constrain the possible initial conditions of the collision and the QGP viscosity. Switching to hard probes, I present the main results on the suppression of particle production at high transverse momenta in heavy-ion collision. I continue the discussion with a few highlights from the beam energy scan program at RHIC aimed to probe the properties of the phase boundary and search for the critical point in the QCD phase diagram. I complete my proceedings with a few remarks on probes of local parity violation in the strong interaction which shows the potential to go beyond the scope of the QGP physics with the heavy-ion programs at RHIC and LHC.

2 Particle yields

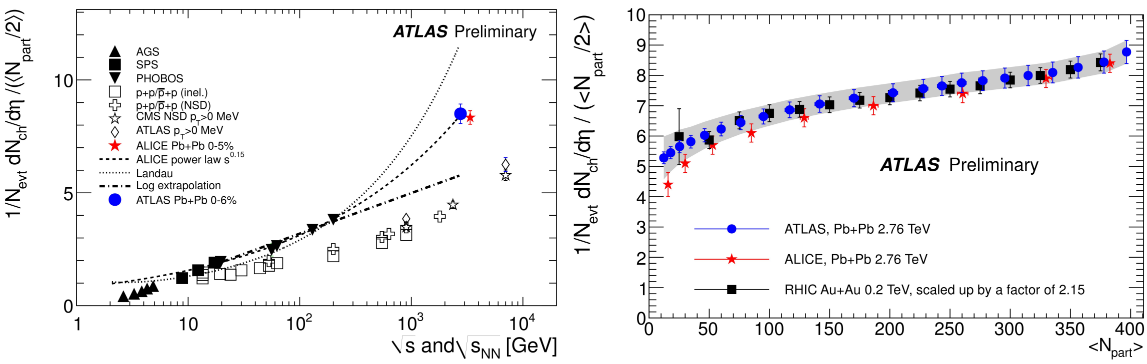

(a) **(b)**

Figure 1: (a) Charged particle multiplicity per participant pair measured for Pb–Pb collisions by the ALICE and ATLAS Collaborations at LHC, and compared to results for proton-proton and heavy-ion collisions at lower energies. (b) Centrality dependence of the multiplicity per participant pair measured by the ALICE and ATLAS Collaborations at the LHC, and the STAR Collaboration at RHIC. Figures taken from [1].

Figure 1(a) shows a compilation of the results for charged particle multiplicity density measured for heavy-ion collisions at the LHC and lower energies at RHIC, SPS, and AGS, as well as for proton-proton collisions. The charged particle multiplicity density in central Pb–Pb collisions at 2.76 TeV/nucleon is measured to be $\mathrm{d}N_{\mathrm{ch}}/\mathrm{d}\eta \approx 1600$, what is larger by a factor of 2.15 than that at top RHIC energy. Compared to pp collisions at the same energy the charge density is increased by a factor of 1.9. The measured multiplicity and spectra correspond to an increase by 2.5-3 times in energy density from RHIC to LHC, which for central Pb–Pb collisions at LHC is measured to be $dE_t/d\eta \sim 2$ TeV per unit of rapidity [2]. As it can be seen from Fig. 1(b) the shape of the charged particle production per participant pair versus centrality is almost identical for RHIC and LHC energies, what may indicate that saturation effects do not significantly change despite shifting toward smaller Feynman x_f at LHC.

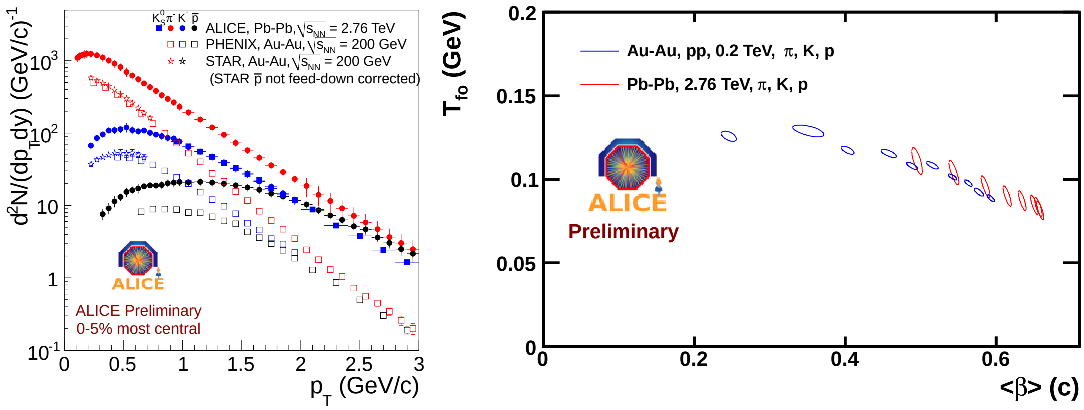

(a) **(b)**

Figure 2: (a) Identified charged particle spectra measured by the ALICE Collaboration for heavy-ion collisions at the LHC in comparison with results for top RHIC energy. (b) Freeze-out temperature, T_{fo}, and radial velocity, $\langle \beta_t \rangle$, extracted from the blast wave fits to the identified charged particle spectra measured at RHIC and LHC. Figures taken from [3].

Figure 2(a) shows the transverse momentum spectra of identified particle measured by the ALICE Collaboration for the 0-5% most central Pb–Pb collisions at 2.76 TeV/nucleon. The spectra slopes change dramatically compared to RHIC data (open symbols in Fig. 2(a)), especially for protons. This reflects a significantly stronger radial flow. The radial flow velocity reaches about 60% of the speed of light with a simultaneous reduction of the kinetic freeze-out temperature down to 80 MeV (Fig. 2(b)).

3 Bose-Einstein correlations

Figure 3 shows the decoupling time and the size of the freeze-out (homogeneity) region of the fireball created in Pb–Pb collisions at LHC and at lower energies. The volume and the

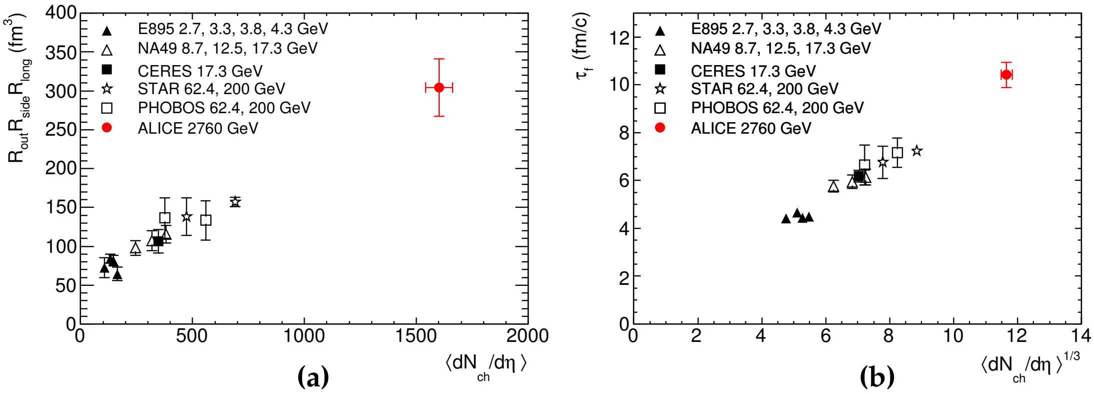

Figure 3: (a) The homogeneity volume (triple product of the pion HBT radii which is proportional to the system volume via $(2\pi)^{\frac{3}{2}}$ coefficient). (b) The decoupling time of the system created in the heavy-ion collision. Results are for Pb–Pb collisions at 2.76 TeV/nucleon measured by the ALICE Collaboration, and for central Au–Au and Pb–Pb collisions for lower AGS and RHIC energies. Figures taken from [4].

system lifetime are deduced from the Hanbury-Brown-Twiss (HBT) momentum-space two-particle correlations of identical pions. The HBT homogeneity region, which is connected to the HBT out- long- and side- radii via $(2\pi)^{\frac{3}{2}} R_{\rm out} R_{\rm side} R_{\rm long}$, increases by a factor 2 (Fig. 3(a)) compared to the top RHIC energy of 0.2 TeV/nucleon pair. The system lifetime also increases by more than 30% (Fig. 3(b)). These trends are consistent with hydrodynamical model calculations for LHC energies using parameters tuned to reproduce the RHIC data.

4 Anisotropic transverse flow

Azimuthal anisotropic flow is a key observable indicating collectivity among particles produced in relativistic heavy-ion collisions. Figure 4 shows the integrated (a) and p_t differential (b) elliptic flow, v_2, measured in Pb–Pb collisions at 2.76 TeV/nucleon. The immediate conclusion to be drawn from the comparison of v_2 results measured at LHC by the ALICE, ATLAS, and CMS Collaborations to that at lower RHIC energies is that the integrated v_2 increases by 30%, see Fig. 4(a). Figure 4(b) shows the differential flow results as a function of charged particle's transverse momentum, $p_{\rm t}$. The results from RHIC and the LHC are similar in both magnitude and the shape of $p_{\rm t}$ dependence. This behavior is a consequence of a stronger radial flow at the LHC as was already discussed in Sec. 2 above. The strong particle collectivity reflected by large v_2 at LHC shows that the system

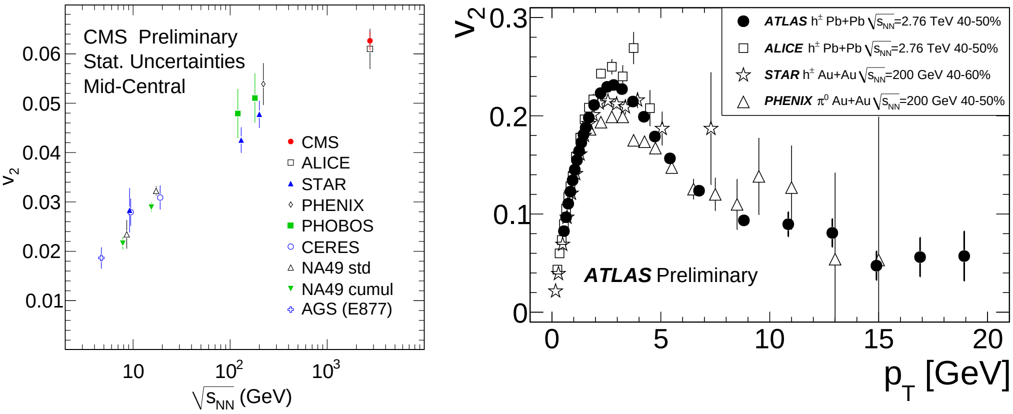

(a) **(b)**

Figure 4: (a) Integrated elliptic flow v_2 as a function of the collisions energy. (b) v_2 as a function of transverse momentum for the 40-50% centrality range measured in heavy-ion collisions at RHIC and LHC. Figure (a) taken from [2], figure (b) from [1].

created in heavy-ion collision at TeV energy scale behaves as a strongly interacting, close to be a perfect fluid - similar to the properties of the QGP observed at RHIC. All this speaks towards applicability of the hydrodynamic model description of the heavy-ion collisions at LHC energies.

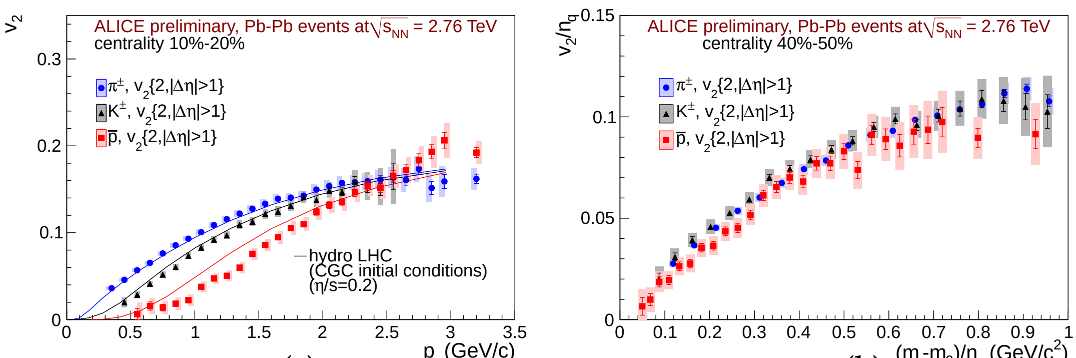

(a) **(b)**

Figure 5: (a) Elliptic flow of pions, kaons and anti-protons vs. transverse momentum for the 10-20% centrality range. The lines are hydrodynamical model calculations. (b) Elliptic flow versus transverse kinetic energy are both scaled with the number of constituent quarks for the 40-50% centrality range. Figures taken from [5].

Qualitatively the validity of the hydrodynamic description for LHC and effects of stronger radial flow can be tested with the anisotropic flow measurement of identified particles and its dependence on the mass of different species. Figure 5 shows the p_t differential elliptic flow of charged pions, kaons, and protons measured by the ALICE Collaboration in Pb–Pb collisions at 2.76 TeV/nucleon. The observed larger than at RHIC mass splitting of v_2 agrees well with a picture of increased radial flow and follows viscous hydrodynamic predictions (solid lines in Fig. 5(a)) except for anti-protons in the most central collisions. Anti-protons also fall out of the universal scaling with number of quarks seen at RHIC energies.

One of the main highlights of recent anisotropic flow results from both RHIC and LHC experiments is establishing the connection between the measured event anisotropy in the momentum space (anisotropic flow) and the fluctuations of the energy density in the initial state of the heavy-ion collisions.

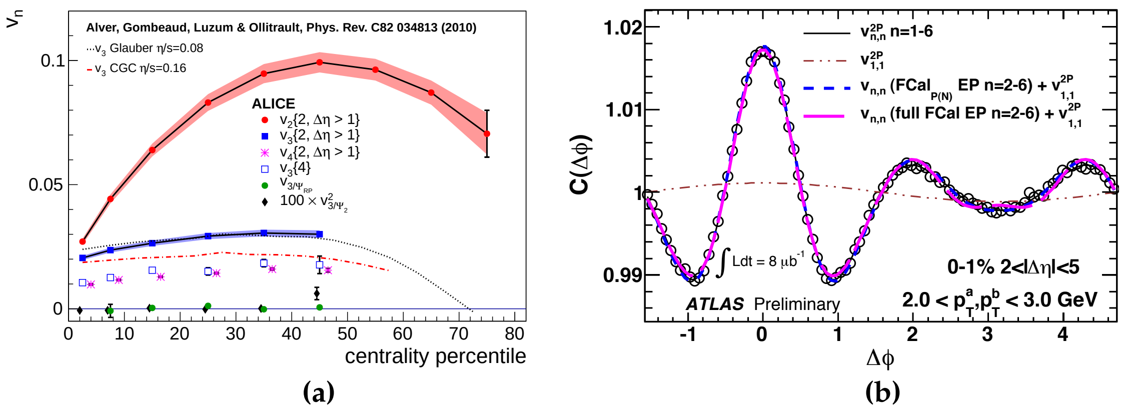

Figure 6: (a) Integrated elliptic (v_2), triangular (v_3), and quadrangular (v_4) flow measured for Pb–Pb collisions at 2.76 TeV/nucleon by the ALICE Collaboration. (b) Two-particle correlation function measured for 1% most central collisions by the ATLAS Collaboration. The measured 2-particle correlations are reproduced well by the combination of the Fourier coefficients from the anisotropic flow measurement (solid lines). Figure (a) taken from [5], figure (b) from [1].

Figure 6(a) shows higher order harmonics of anisotropic flow (v_3, v_4) together with the largest v_2 component for Pb–Pb collisions at 2.76 TeV/nucleon measured by the ALICE Collaboration. The geometrical origin of the v_3 component is established by comparison of the vanishing triangular flow, v_3, when measured with respect to the collision reaction plane (green symbols in Fig. 6(a)), vs. non-zero v_3 measured with respect to the participant plane - the plane determined by the event-by-event fluctuating shape of the initial energy density (blue squares in Fig. 6(a)). Triangular and higher order harmonic flow also explains the double hump structure seen originally at RHIC in the two-particle azimuthal correlations and often referred to as the Mach Cone effect. Figure 6(b) shows that for the most central Pb–Pb collisions at 2.76 TeV/nucleon the whole shape of the two particle azimuthal correlations is driven by the interplay between various anisotropic flow components, mainly v_2 and v_3.

5 Particle production at large transverse momenta

Production of particles with very large transverse momentum, p_t, in heavy-ion collisions happens very early in the collision history and therefore these particles have to propagate through the hot and dense medium created in the collision. Consequently, the modification of high p_t particle production compared to the production without medium (e.g. in proton-proton collisions) carries information about the medium properties such as the energy loss mechanism and its dependence on the path length. Quantitatively the modification of particle production is described by the nuclear modification factor, R_{AA}, which presents the ratio of the particle yields in heavy-ion collision to that of the proton-proton collisions scaled by the corresponding number of binary collisions. Figure 7(a) shows the charged particle

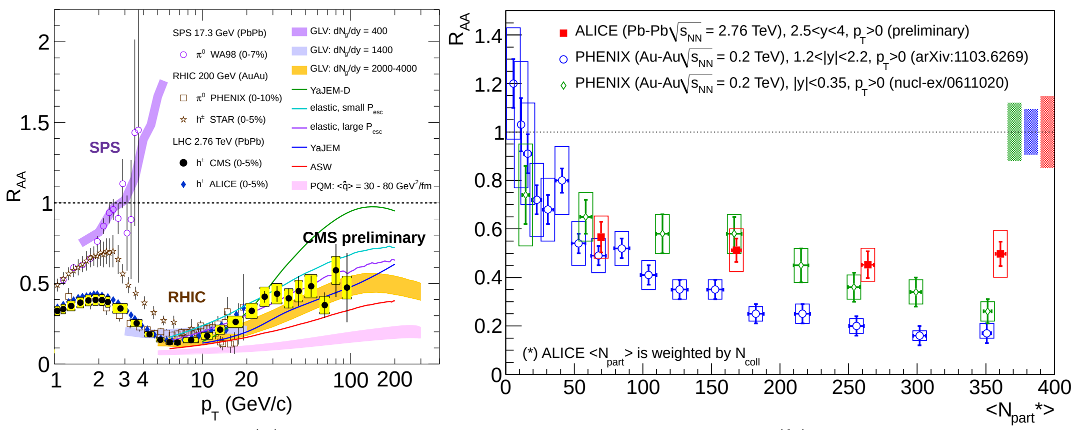

(a) **(b)**

Figure 7: (a) Nuclear modification factor, R_{AA}, as a function of transverse momentum for neutral pions and charged hadrons for the most central heavy-ion collisions. (b) R_{AA} of J/ψ as a function of the number of participants measured at RHIC and LHC. Figure (a) taken from [2], figure (b) from [8].

nuclear modification factor, R_{AA}, for Pb–Pb collisions at 2.76 TeV/nucleon measured by the ALICE and CMS Collaborations compared to results for charged and identified neutral pions from RHIC and SPS experiments. The deviation of R_{AA} from unity reflects the effect of medium modification, and reveals strong suppression ($R_{AA} << 1$) of particle production in heavy-ion collisions compared to that in proton-proton interactions. As a function of transverse momentum, R_{AA} shows a minimum around 5-7 GeV/c, and then rises significantly towards higher transverse momentum but even at $p_t \sim 100$ GeV/c the particle production is largely suppressed ($R_{AA} \sim 0.5$). Compared to different model calculations (color lines in Fig. 7(a)) these new results provide strong constrains on models with different parton energy loss. Figure 7(b) shows that even heavy quark (J/ψ) production is strongly suppressed at RHIC and LHC, though at LHC the suppression is reduced in accord with the expectations from the statistical model [9].

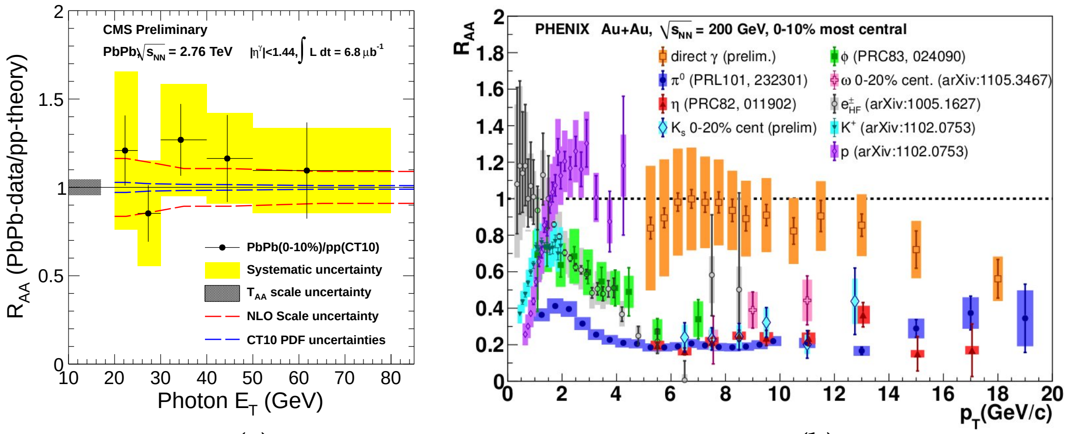

(a) **(b)**

Figure 8: (a) Nuclear modification factor, R_{AA}, of isolated photons as a function of transverse momentum for 0-10% central events measured by the CMS Collaboration. (b) Results by the PHENIX Collaboration for R_{AA} of several mesons and direct photons for the 0-10% central Au–Au collisions. Figure (a) taken from [2], figure (b) from [7].

Important probes of the nuclear parton densities created in heavy-ion collision are the colorless objects such as prompt photon and Z boson, since they are produced directly from hard parton interactions and propagate through the medium of quarks and gluons without modification. Figure 8(a) shows the R_{AA} of direct photons as a function of the photon transverse energy for the most central Pb–Pb collisions measured by the CMS Collaboration. Photon R_{AA} measured at LHC is consistent with unity (no modification), which is similar to the recent results for prompt photons by the PHENIX Collaboration (orange points in Fig. 8(b)). The R_{AA} of another colorless probe, the Z boson, is also measured by the CMS Collaboration and found to be consistent with no medium modification: $R_{\mathrm{AA}}^{(Z)} = 1.2 \pm 0.29(\mathrm{stat.}) \pm 0.16(\mathrm{syst.})$ [10].

6 RHIC beam energy scan and the search for the critical point

Another frontier of the heavy-ion physics program, which complements the study of the QGP properties at RHIC and LHC, is to determine the nature of the phase transition between confined (hadrons) and deconfined (quark-gluon plasma) matter with a search for the critical point on the QCD phase diagram. These two objectives are the main goals of the Beam Energy Scan program at the RHIC facility. The features of the phase transition and proximity of the critical point can be studied by looking at irregular changes in the degrees of freedom of the system created in heavy-ion collisions. Experimentally this should be reflected in non-monotonic behavior of the sensitive physics observables. Examples of sensitive observables are particle collectivity such as anisotropic flow or HBT correlations, or fluctuations in the system (e.g. fluctuations of the conserved quantities such as baryon number or strangeness).

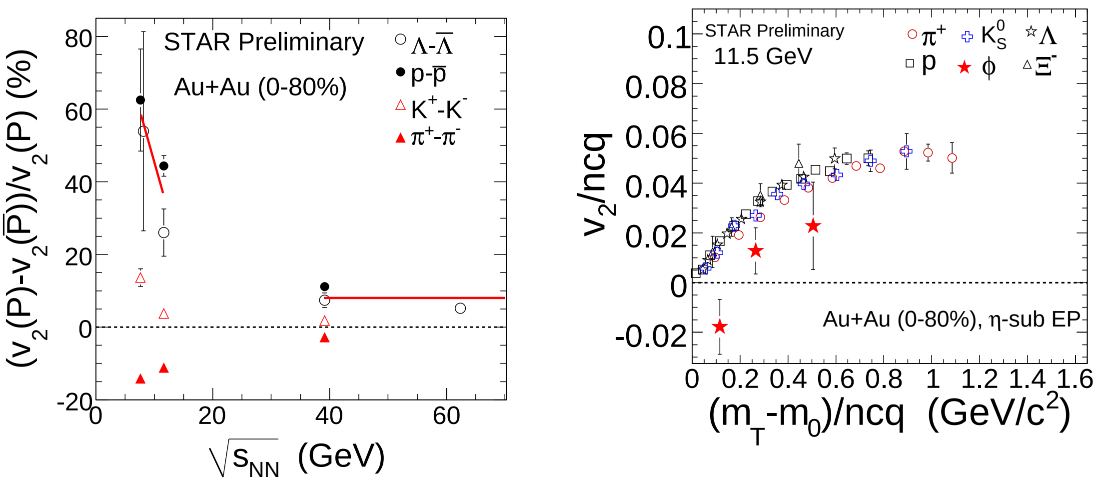

(a) **(b)**

Figure 9: (a) Fractional difference between elliptic flow of particles and anti-particles for 0-80% Au–Au collisions plotted vs. collision energy. (b) Elliptic flow of identified particles for Au–Au collisions at 11.5 GeV/nucleon versus transverse kinetic energy both scaled by the number of constituent quarks. Figures taken from [11].

Figure 9(a) shows the relative variation in the identified particle and anti-particle elliptic flow measured by the STAR Collaboration for different collision energies ranging from 11.5 GeV/nucleon up to the top RHIC energy of 200 GeV/nucleon. With decreasing collision energy the baryon and anti-baryon elliptic flow difference increases dramatically compared to that for mesons. Another change in the elliptic flow patter at lower energies is the breaking of the constituent quark scaling for the elliptic flow which seems to hold at top RHIC energy. Figure 9(b) shows number of constituent quark scaled elliptic flow of identified particles for Au–Au collisions at 11.5 GeV/nucleon. Despite the large statistical errors, results for the ϕ-meson (which carries the information about the strange quark production) deviates significantly from the overall scaling of other particles, which probably indicate the breaking of the quark collectivity at lower energies and change in the degrees of freedom in the system.

Figure 10(a) shows results for the higher order moments (the skewness, S, and kurtosis, κ) of the net proton number. Small deviation of the conserved quantity, the baryon number, from the Hadron Gas Resonance (HGR) model below 39 GeV/nucleon may suggest a hint of proximity to the critical point. Figure 10(b) shows the charged particle R_{AA} down to

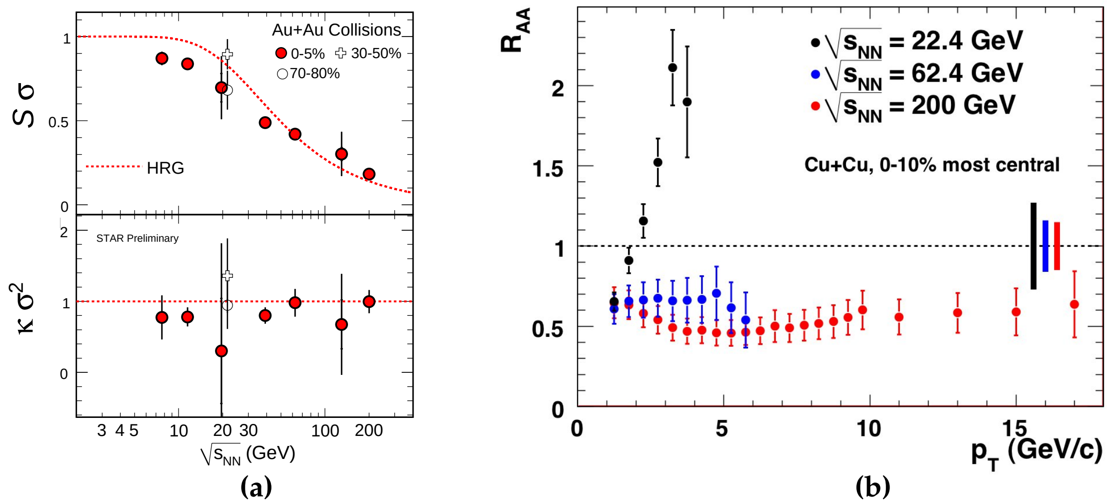

Figure 10: (a) Higher order moments of the net proton number vs. collision energy. (b) The nuclear modification factor of neutral pions as a function of transverse momentum for Cu–Cu collisions at three different energies. Figure (a) taken from [11] and figure (b) taken from [12].

an energy of 22.4 GeV/nucleon and it illustrates the significant change in pattern of the particle suppression at lower energy compare to the top RHIC energy. Overall, there are some hints from the Beam Energy Scan program at RHIC on the possible critical point between energies of 7 and 20 GeV/nucleon. Hopefully the upcoming measurements from RHIC energy scan will allow us to make a conclusive statement about existence of the QCD critical point.

7 Probes of local parity violation in strong interactions

The strong magnetic field created in the interaction zone of non-central relativistic heavy-ion collisions may interact with the topologically non-trivial gluonic field configurations of QCD such as instantons and sphalerons. It is predicted [13] that experimentally this may lead to charge separation of hadrons produced in the collision along the magnetic field, which itself is aligned perpendicular to the reaction plane of the collision. Since instanton and sphaleron configurations breaks the parity symmetry of QCD, the measurement of charge separation provides a unique experimental test of how well the parity symmetry is preserved by the strong interaction [14].

Experimentally the effects of charge separation can be quantified by the charge dependent azimuthal correlations with respect to the reaction plane. Figure 11 shows the experimental results for the $\langle \cos(\phi_\alpha + \phi_\beta - 2\Psi_{RP}) \rangle$ correlator, which is the parity even observable but

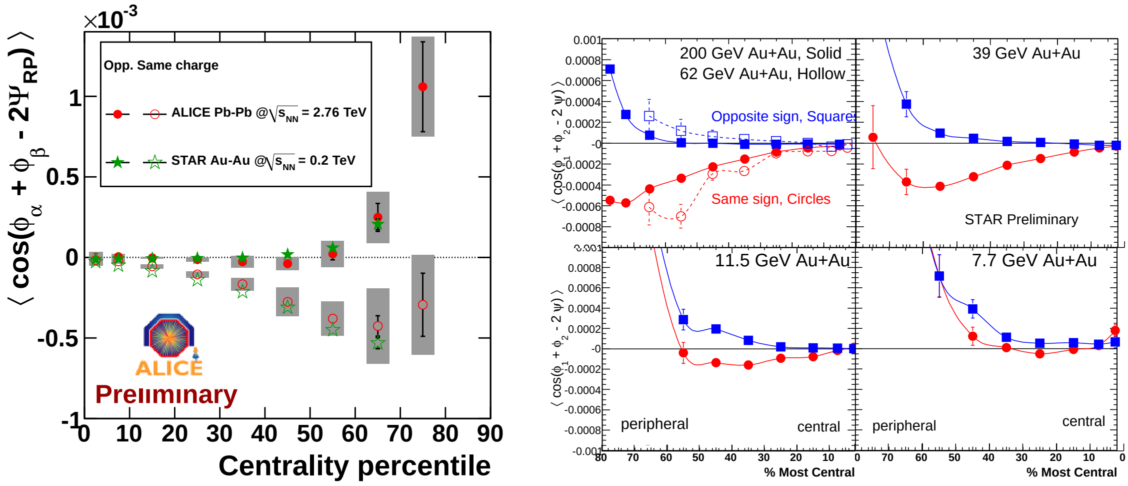

(a) **(b)**

Figure 11: Charged dependent azimuthal correlations with respect to the reaction plane of heavy-ion collision vs. centrality: (a) comparison between results for Pb–Pb collisions at 2.76 TeV/nucleon vs. the measurement for Au–Au at 200 GeV/nucleon, (b) results for Au–Au collisions for 5 different collision energies in the range of 7.7 - 200 GeV/nucleon. Note the inverted centrality scale in figures (a) and (b). Figure (a) taken from [15] and figure (b) from [11].

directly sensitive to the event-by-event charge fluctuations, and thus to the possible local parity violation in strong interactions. The STAR and PHENIX Experiments at RHIC, and now the ALICE Collaboration at LHC [15] observe a significant charge separation at higher collision energies (Fig. 11(a)), which seems to disappears between 11.5 and 7.7 GeV energies (lower panel in Fig. 11(a)). The experimental situation is significantly complicated by the presence of the parity conserving background correlations which may contribute to the measured charge dependent azimuthal correlations at RHIC and LHC. Recent progress in understanding the possible parity even backgrounds, such as identifying the large flow fluctuations in the first harmonic flow helps to better understand background contributions, but there is still a long way to go before we will be able to conclude whether the observed charge separation is indeed connected to the effects of local parity violation, or it is just a complicated interplay of yet unidentified background sources.

8 Summary

The results by the ALICE, ATLAS, and CMS Collaborations from the first heavy-ion run at the Large Hadron Collider in November 2010 opened a new era of experimental studies of the quark-gluon plasma in the laboratory. Together with the new high statistics data collected during the past few years by the STAR and PHENIX Experiments at the Relativistic

Heavy Ion Collider this provides an extremely rich experimental data set which allows us to study the properties of the quark-gluon plasma in the great detail, and let us to learn more about the features of the universe a few microseconds just after the Big Bang. I am looking forward to further experimental developments and more exciting results from the LHC and RHIC scientific communities!

References

[1] P. Steinberg [ATLAS Collaboration], arXiv:1107.2182 [nucl-ex].

[2] B. Wyslouch [CMS Collaboration], arXiv:1107.2895 [nucl-ex].

[3] M. Floris [ALICE Collaboration], arXiv:1108.3257 [hep-ex].

[4] K. Aamodt *et al.* [ALICE Collaboration], Phys. Lett. **B696** (2011) 328-337.

[5] R. Snellings [ALICE Collaboration], arXiv:1106.6284 [nucl-ex].

[6] A. Adare *et al.* [PHENIX Collaboration], arXiv:1105.3928 [nucl-ex].

[7] D. Sharma [PHENIX Collaboration], Proceeding of Quark Matter 2011 Conference: `http://www.phenix.bnl.gov/phenix/WWW/publish/deepali/qm2011/proceedings.pdf`.

[8] G. Martinez Garcia [ALICE Collaboration], arXiv:1106.5889 [nucl-ex].

[9] A. Andronic, P. Braun-Munzinger, K. Redlich, J. Stachel, arXiv:1106.6321 [nucl-th].

[10] Y. -J. Lee [CMS Collaboration], arXiv:1107.2131 [hep-ex].

[11] B. Mohanty [STAR Collaboration], arXiv:1106.5902 [nucl-ex].

[12] M. L. Purschke [PHENIX Collaboration], Proceeding of Quark Matter 2011 Conference: `http://www.phenix.bnl.gov/phenix/WWW/publish/purschke/qm2011/purschke_proc_vers3.pdf`.

[13] D. E. Kharzeev, L. D. McLerran and H. J. Warringa, Nucl. Phys. A **803**, 227 (2008).

[14] S. A. Voloshin, Phys. Rev. **C70**, 057901 (2004).

[15] P. Christakoglou [ALICE Collaboration], arXiv:1106.2826 [nucl-ex].